Mathematical Modeling and Algorithm Application
ISSN: 3006-0842 | Vol. 5, No. 3, 2025

Integration of Mechanical Properties and Stability Index for the Stability Analysis of Tunnel Surrounding Rocks in a Deep Coal Mining Environment

Md Jahid Hasan[1], Davie Jaja[2]

[1]School of Civil Engineering, Henan Polytechnic University, Jiaozuo, Henan, China
[2]School of Safety Science and Engineering, Henan Polytechnic University, Jiaozuo, Henan, China

Abstract: This study investigates the mechanical properties and stability classification of surrounding rock masses in deep coal mine roadways using the Guojiawan Coal Mine in Shanxi Province, China, as a case study. This study synthesized multiple parameters from laboratory testing, in situ stress measurements, and the Stability Index (SI) method to quantify stability by lithology type in a heterogeneous deep mining system. The study developed a procedure that involved collecting rock samples from the 51206 and 51207 return ventilation roadways that represented silty mudstone, fine sandstone, coarse sandstone, and coal, and utilizing the GB/T 23561.1-2009 specifications, the samples were tested using uniaxial compressive, Brazilian splitting, and triaxial compressive testing. Statistical analysis ($n \geq 3$ for each test type) of the rock samples showed that coarse sandstone had the highest uniaxial compressive strength (UCS) (52.86 ± 1.85 MPa) and elastic modulus (13.11 ± 0.75 GPa), and coal had the lowest (UCS: 20.43 ± 2.15 MPa; E: 2.36 ± 0.22 GPa). In situ stress conditions were low to moderate (σH = 9.99 MPa at 270 m); however, localized stress concentrations were present next to lithologies. The SI classified coarse sandstone as stable (e = 0.30-0.44), silty mudstone as stable to moderately stable (e = 0.47-0.73), and coal seams as moderately stable (e = 0.31-0.46). The Guojiawan Coal Mine case study illustrates how using laboratory-derived parameters together with site-specific stress conditions can provide results to optimize roadway support design in deep and geologically heterogeneous mining environments, offering a transferable framework for similar underground excavations.

Keywords: Rock Mechanics, Tunnel Stability, Uniaxial Compressive Strength, Stability Index, Deep Coal Mining, In-Situ Stress

1. Introduction:

As shallow resources are depleted, the mining industry is faced with increasingly deeper and deeper underground coal mining projects. The in-situ stress-related issues, ground pressure, are also related to rock burst, and the stability of surrounding rock in greater depth tunneling becomes more difficult [1], [2], [3], [4], [5]. As the depth associated with the mining operation increases, the complexity of the mechanical behavior of rock mass and the redistribution of stress around the excavation increases[6], [7], [8], [9], [10], [11]. The stability of the surrounding rock associated with the tunnels is a crucial aspect of mining operations pertaining to health and safety and productivity [12], [13], [14]. Rock instability can cause mine downtime, damage to mine infrastructure, and a significant safety risk [15], [16], [17]. Therefore, determining and quantifying the mechanical parameters associated with rock mass, such as uniaxial compressive strength, tensile strength, cohesion, friction angle, and Young's modulus, is useful when designing and optimizing roadway supports as well as the roadway excavation scheme [6], [18], [19], [20]. More work has been done on the mechanical behavior of the surrounding rock that is associated with deep roadways and the failure mechanisms. Cai et al.[21] investigated high-stress concentration zones near excavation boundaries, and Shi& Zhang. [22]ddiscussed the characterization of failure zones to describe some of the rock deformation behavior. The Stability Index method, first developed by Barton[23] and built upon by others, offers a systematic methodology to numerically rank the rock mass quality and obtain some estimates of the support provided at depth. In this paper, we evaluate the deep mining tunnel at the Guojiawan Coal Mine Second Panel, which is noted for its geological and stress states and is representative of the challenges related to deep mining conditions. Laboratory testing of the intact and distressed rock samples removed from the site provided the opportunity to study the mechanical behavior of the surrounding rock under simulated field conditions[24]. The objective of this research analysis is to examine the mechanical responses, define the mechanical parameters, and assess the stability of the tunnel by using the Stability Index method[18]. This paper uniquely merges in situ stress measurements, laboratory mechanical testing, and Stability Index classification into one study of site stability for the Guojiawan Coal Mine-the first such dataset for this site. An unusual discover has also emerged: the low friction angle of the high-strength coarse sandstones, implying latent shear weaknesses. The derived results furnish lithology-level stability thresholds that can be directly used in the roadway support design of environments in deep coal mining.

2. Experimental Method

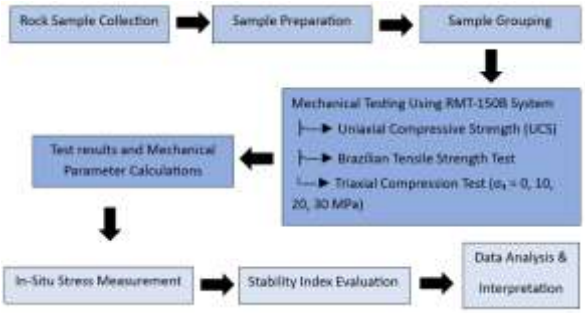

Figure 2-1 Workflow Diagram

2.1. Rock Sample Collection and Preparation

Samples were obtained from the roadway sections of the Guojiawan Coal Mine. Fine to medium-coarse grained sandstone, silty mudstone, and various coal samples were analyzed in the paper. Sampling complied with the Chinese national standard GB/T 23561.1-2009,

Cylindrical samples with diameters of Φ50 mm × 100 mm for tensile strength test disc-shaped specimens with a diameter of Φ 50 mm × 25 mm

To retain the natural structure and integrity of the rock mass as well as properly characterize the mechanical properties, the samples were retrieved in the field directly from the tunnel. Detailed records were kept for each sample with exhaustive information, including the sample identification number, lithology, stratigraphic unit, and stratum thickness. Comprehensive records were maintained throughout the process.

2.2. Testing Equipment and Grouping.

All the mechanical tests were made using the RMT-150B electro-hydraulic servo rock testing machine. This machine can deliver an axial force of 2000 kN, and confining pressures of up to 60 MPa can be applied. Digital displacement meters, as well as high-precision load cells, were installed in the testing machine, allowing for the precise determination of the stress–strain behavior.

Rock samples retrieved in the tunnel ceiling from 51206 and 51207 return air roadway were converted into normalized cylinders, henceforth grouped into groups A to I. The return air roadway drill core roof rock samples were divided into four groups, and the 51206-return air roadway drill core roof rock samples were divided into five groups. At least three specimens were applied in the uniaxial compression tests, while at least five were used in the Brazilian splitting and triaxial compression tests to improve the accuracy of the findings.

Figure 2-2 Mining Faces in the Second Panel Area

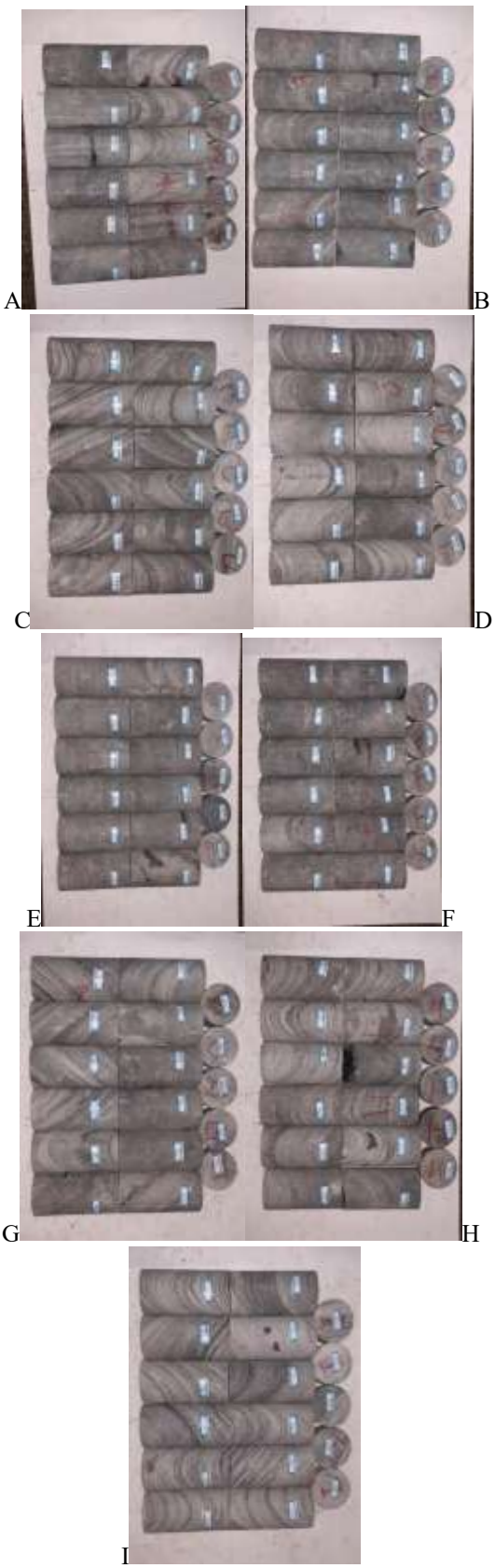

Figure 2-3 Prepared rock samples for testing from 51206 and 51207 return air roadway

2.3. Determination of Mechanical Parameters

The mechanical behavior of the surrounding rock was assessed using standard laboratory tests. As for calculate the stability Index of for the Stability Index Classifications use this following equation:

Stability Index.

$e = \sigma_\theta / \sigma_r$

$\sigma_r = 0.7.\sigma_c$

σ_θ =maximum stress around the tunnel

σ_r =long-term resistance strength

σ_c =compressive strength (UCS) of the specific rock type.

< 0.5 → Stable

0.5 – 1.2 → Moderately Stable

1.2 – 2.5 → Unstable

> 2.5 → Extremely Unstable (Strong Rheology)

These parameters collectively describe the strength, deformation characteristics, and stability of the surrounding rock formations."

3. Results and Analysis

3.1. Results

Figure 3-1 Coal Samples after the mechanical parameter tests from 51207

Figure 3-2: Results of Uniaxial compression failure test of roof rock samples from 51207 return airway

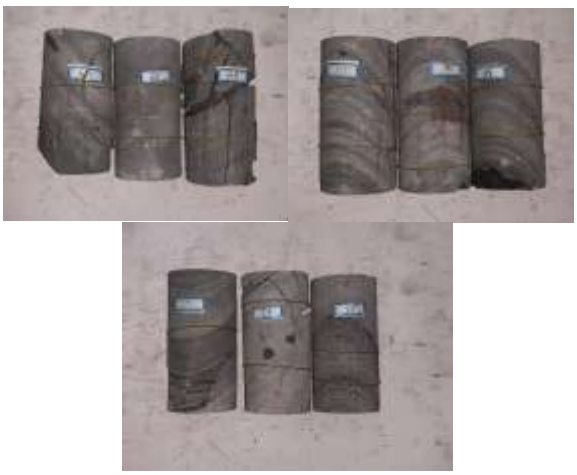

Figure 3-3: Roof rock samples after Uniaxial compression failure test from 51206 return airway

Figure 3-4: After the Brazilian splitting test of roof rock samples from 51207 return airway

Figure 3-5: After the Brazilian splitting test of roof rock samples from 51206 return airway

Figure 3-6: Roof rocks condition after Triaxial compression test from 51207 return airway

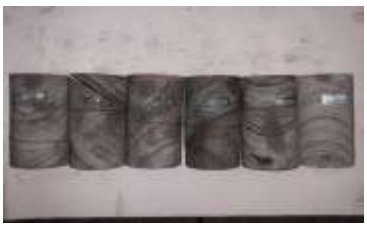

Figure 3-7: Roof rocks condition after Triaxial compression test from 51206 return airway

Table 3-1: Physical and mechanical parameters of roof rocks in 51207 return airway

Rock Type	ρ-g/cm³	UCS(MPa)	TS(MPa)	E(GPa)	Ed(GPa)	S-UC(MPa)	V	C(MPa)	φ (°)
Fine Sandstone	2.468	33.401	1.828	12.318	9.097	6.655	0.271	18.85	39.9
Fine-Grained Sandstone	2.513	35.448	1.490	9.242	7.66	10.305	0.103	22.056	22.4
Coarse-Grained Sandstone	2.53	51.487	3.377	16.018	10.251	16.318	0.17	25.362	17.7
Fine Sandstone	2.431	39.377	3.303	10.966	6.693	8.123	0.159	17.559	28.3

Table 3-2: Physical and Mechanical Parameters of Roof Rock in the 51206 Return Air Roadway

Rock Type	ρ-g/cm³	UCS(MPa)	TS(MPa)	E(GPa)	Ed(GPa)	S-UCS(MPa)	V	C(MPa)	φ (°)
Silty Mudstone	2.496	32.272	2.947	9.527	8.781	6.792	0.048	11.961	30.5
Fine-Grained Sandstone	2.474	41.345	1.829	11.035	10.275	2.407	0.213	17.059	25.5
	2.487	41.253	1.134	9.912	8.906	9.558	0.222	21.624	19.2
	2.454	37.896	2.1	10.236	7.869	25.786	0.070	4.885	44.2
Coarse-Grained Sandstone	2.432	52.862	2.157	13.105	10.831	27.726	0.225	16.558	23.7
Coal	1.293	20.43	0.188	2.36	2.017	12.220	0.312	11	27.2

ρ (g/cm³) → Apparent Density, UCS (MPa) → Uniaxial Compressive Strength, TS (MPa) → Tensile Strength, (GPa) → Elastic Modulus, Ed (GPa) → Deformation Modulus, S-UCS (MPa) → Saturated Uniaxial Compressive Strength, ν → Poisson's Ratio, C (MPa) → Cohesion φ (°) → Friction Angle

3.1.1. Characteristics of the Geostress Distribution

According to existing geostress test results from hydrofracturing, the test results from three measurement points in the 51207-machine head chamber of the Guojiawan Coal Mine, and the geostress testing results from the return air roadway, presented in Table 3-3, the structural stress coefficient is 1.48, which indicates that this sample belongs to a regional modern low-level stress field.

Table 3-3: In-situ stress measurement results at monitoring point 51204

Point	Depth(m)	Σv(MPa)	σH(MPa)	Σh(MPa)	Azimuth σH
1	120	3.24	4.85	3.66	N11.2E
2	120	3.24	4.85	3.53	N9.8E
3	120	3.24	4.53	3.45	N9.9E

Utilizing the contour map of the floor of the 5-1 coal seam in the Erpan area as well as the surface elevation, we determine that the maximum burial depth of the Erpan area is 270 m. The vertical stress is 6.75 MPa, whereas the maximum horizontal stress is 9.99 MPa.

3.1.2. Tunnel Surrounding Rock Stability Analysis

The surrounding rock stability index method is used to assess the overall stability of the mining roadway. This method utilized the ratio of the maximum surrounding rock stress to the long-term strength of the surrounding rock as the stability index and then the stability degree of the surrounding rock was determined based on the stability index.

Table 3-4: Fundamental mechanical parameters of coal and rock masses

Type	ρ(kg/m³)	UCS (MPa)	TS (MPa)	Cohesion (MPa)	φ (°)
Coal	1.29	20.43	0.19	2.63	27.2
Immediate Roof - Silty Mudstone	2.49	32.30	2.95	5.68	30.5
Immediate Roof – Fine Sandstone	2.47	33.40	1.83	18.85	39.9
Coarse Grained Sandstone	2.53	51.50	3.38	25.36	17.7

Therefore, the stability index is as follows:

Silty mudstone (direct roof): e = 0.44-0.66, stable to moderately stable

Coal seam (direct roof): e = 0.70-1.05, moderately stable to

moderately stable

Coarse sandstone (basic roof): e = 0.28-0.42, stable

Fine Sandstone (direct roof) e= 0.43-0.64 (Stable to moderately stable)

3.2. Analysis

Figure 3-8: Mechanical Performance graph of roof rock samples from 51206 and 51207 return air roadway by lithology

The test results show that the lithology of the site clearly controlled the mechanical properties of the surrounding rocks in the Guojiawan Coal Mine. The properties of the coarse sandstone were consistently higher, with the highest values for uniaxial compressive strength (UCS: 52.86 MPa in 51206; 51.49 MPa in 51207) and tensile strength (up to 3.38 MPa), as well as high stiffness (E≈ 13-16 GPa) and average Poisson's ratios (0.17 - 0.23). The higher UCS and tensile strength values indicate that coarse sandstone, under stress, has a load-bearing capacity and deformation that the other lithologies could not compare with. Coarse sandstone was also the most stable rock lithology for tunnel roofs; however, it did present lower friction angles (17.7°), which indicates a lower resistance to shear deformation and displacement path when subjected to complex stress paths. This is relevant for cases where seismic or dynamic loads may be experienced. Fine-grained sandstone provided moderate UCS (35.45-41.35 MPa) and variable tensile strength (1.13-3.30 MPa), and stiffness values were generally (9-12 GPa); it had greater Poisson's ratios about (ν≈0.225) and, compared to coarse sandstone, a greater tendency for lateral expansion under load. The moderately stable performance of fine-grained sandstones also suggested that it could be sensitive to particular structural conditions, and as such, supplemental support may be necessary at some sites. Find-Sandstone have a similar stiff property of Fine-grained sandstone (E = 11.04 GPa, Ed = 10.28 GPa, ν = 0.213) each have moderate Poisson's ratio which may indicate a desirable moderate deformation profile for stable excavation

Silty mudstone attained unconfined compressive strength (UCS) values of about 32 MPa and tensile strength of up to 2.95 MPa, and has moderate stiffness (E ≈ 9.5 GPa) with a very low Poisson's ratio (0.048). A low Poisson's ratio indicates that this is a brittle material, where fracture occurs without forewarning. However, with a high friction angle (30.5–44.2°), there are considerable shear resistive properties which are useful for layered formations in terms of shear stability.

Coal was the weakest material (UCS: 20.43 MPa; TS: 0.19 MPa; E ≈ 2.36 GPa) and most deformable (ν = 0.312). The cohesion was low (2.63–11 MPa) with a moderate friction angle (27.2°), so it exhibited a ductile response under load, albeit displaying poor overall stability, and was the most vulnerable lithology in the tunnel system.

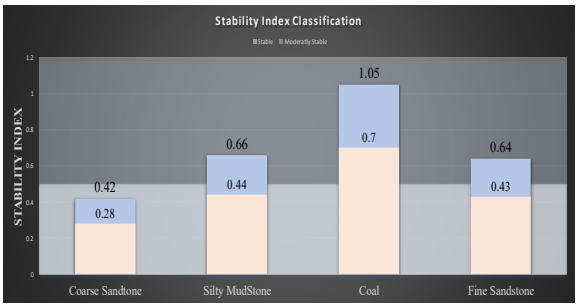

Figure 3- 9: Graph of Stability Index parameters of roof rock samples from 51206 and 51207 return air roadways

Stability Index (SI) classification results support these claims: coarse sandstone is stable (e = 0.28–0.42), silty mudstone is stable to moderately stable (e = 0.44–0.66), coal is moderately stable (e = 0.70–1.05) and, Fine Sandstone is stable to moderately stable (e=0.43-0.64). These classifications align with observed mechanical performance and field observations, providing a quantitative framework for targeted support design.

4. Discussion

The results of this study highlight that lithology is the most significant factor influencing the stability of tunnels surrounding rocks in a deep coal mining setting. Among the tested lithologies, the most significant lithology tested was coarse-grained sandstone with the greatest uniaxial compressive strength (UCS) of up to 52.86 MPa and elastic moduli of 13 and 16 GPa. These results indicate both a great ability to bear loads and high stiffness. The results of this study align with the previous experiments conducted by Kang et al.[1] and Chang et al. [6]; both studies confirmed that coarse sandstone is a dependable self-supporting roof at low-to-moderate stresses, however, the low friction angle (17.6°) urge that, although the sandstone is excellent at bearing compressive loads, it is more susceptible to experiencing shear displacement along weakness planes. It supports Barton's [23] suggestion that high-cohesion, low-friction materials are more likely to undergo shear displacement along weakness planes.

Fine-grained sandstone exhibited moderate unconfined compressive strength (UCS) (35 - 41 MPa), and tensile strength values with significant variability likely attributed to differences in grain size, the quality of cementation and densities of microfracs. This variability replicates the findings of Ni et al. [25] on cyclic strength fluctuations exhibited by

sandstone rocks under cyclic loading. Poisson's ratio is accordingly higher for fine-grained sandstone than for the coarse one, thus reflecting higher lateral expansion under stress, which may favour spalling in unsupported sections.

Silty mudstone had moderate compressive strength (≈32 MPa) but had the highest friction angles of the lithologies measured (30.5 - 44.2°); this suggests strong shear resistance, increasing stability in layered formations. However, a very low Poisson's ratio (0.048) indicates brittle behaviour, and ultimately suggests failure will occur catastrophically when it exists under adverse redistribution. The findings from this research support Wang et al.[26]'s findings that classified brittle fracture as one key risk regarding working with silty mudstone in the context of tunnels and deep construction.

The weakest of lithologies turns out to be coal, with low UCS (20.43 MPa), tensile strength (0.19 MPa), and stiffness (E ≈ 2.36 GPa), coupled with the highest Poisson ratio (ϑ = 0.312). The low strength and high deformability caused mainly roof sagging and sidewall deformation when juxtaposed against stiffer lithologies such as sandstone, as also mentioned by Fan et al.[27]. Differential deformation and stress concentration arise from basinal coal layers adjacent to harder strata, accentuating the potential for localized failure.

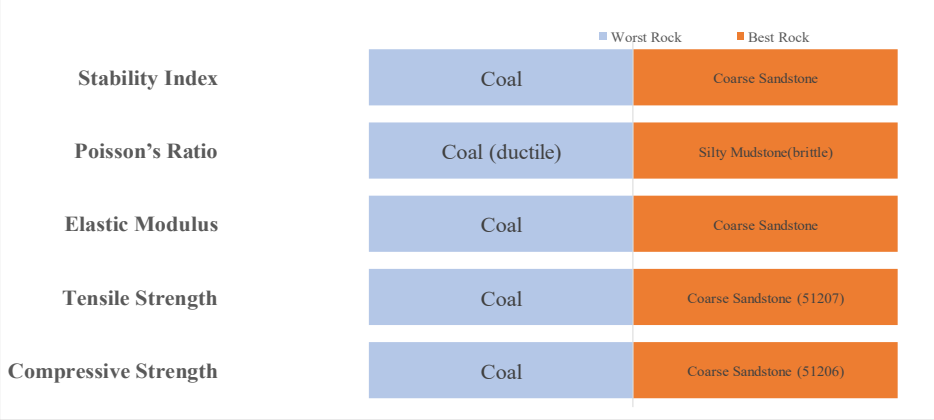

Figure 4-1: Worst and Best rocks base on the experiment results of their mechanical performance

In practical terms, the Stability Index (SI) method classifies coarse sandstone as stable (e = 0.28–0.42), silty mudstone as stable to moderately stable (e = 0.44-0.66), coal as moderately stable (e = 0.70–1.05) and Find Sandstone as stable to moderately stable (e=0.43-0.64). These classifications align the SI with laboratory-derived mechanical properties and field observations of deformation patterns. The integration of laboratory- and field-based SI assessment harmoniously contributes to a schematic for designing support configurations: slight reinforcement in the coarse sandstone zone, stiff and continuous support to the brittle silty mudstone layers, and rigid high-capacity systems (bolt–mesh–anchor or grouting) in coal-bearing zones.

Surprisingly, a low friction angle of coarse sandstone, even with very high strength and cohesion, must be further explored. A plausible explanation might be mineral alignment or micro-crack networks that reduce shear resistance. Similarly, the fairly high variability in fine-grained sandstone strength values shows that localized variability matters more than initially thought.

Limitations and Future Research:

The study only contained data from a single location with a low to moderate in situ stress reign; so extra care should be taken when generalizing these results in geological settings with high stress.

The aforementioned limitations may be addressed in the future, namely, by expanding the dataset to include more deep mining sites under different lithology and stress conditions. Numerical modelling approaches such as FLAC3D or UDEC could simulate time-dependent deformation, especially in heterogeneous portions containing coal–sandstone interfaces. Long-term monitoring procedures, such as acoustic emission and microseismic methods, may provide clues for early warnings of instability to validate the predictions made using the Stability Index through time.

5. Conclusion

Therefore, this paper confirms that the lithology dominates tunnel stability in deep coal mining conditions. It combines mechanical property testing with in situ stress measurement and SI classification to suggest a road support design decision-making tool that is of immediate engineering value and thus may facilitate more detailed predictive modelling later.

References

[1] H. Kang, F. Gao, G. Xu, and H. Ren, “Mechanical behaviors of coal measures and ground control technologies for China’s deep coal mines – A review,” J. Rock Mech. Geotech. Eng., vol. 15, no. 1, pp. 37–65, Jan. 2023, doi: 10.1016/j.jrmge.2022.11.004.

[2] S. Luo et al., “Stability Index of Surrounding Rock during Deep Rock Excavation Considering Energy Release Speed,” Appl. Sci., vol. 13, no. 5, p. 3000, Feb. 2023, doi: 10.3390/app13053000.

[3] K. Hou, M. Zhu, Y. Hao, Y. Yin, and L. An, “Stability analysis and evaluation of surrounding rock of ultra-deep shaft under complicated geological conditions,” Front. Earth Sci., vol. 11, p. 1216667, July 2023, doi: 10.3389/feart.2023.1216667.

[4] J. A. Hudson and J. P. Harrison, Engineering rock mechanics: an introduction to the principles, Repr. Oxford [u.a.]: Pergamon, 2007.

[5] B. H. G. Brady and E. T. Brown, Rock mechanics: for underground mining, 3rd ed. Dordrecht ; Boston: Kluwer Academic Publishers, 2004.

[6] J. Chang, K. He, Z. Yin, W. Li, S. Li, and D. Pang, “Study on the Instability Characteristics and Bolt Support in Deep Mining Roadways Based on the Surrounding Rock Stability Index:

Example of Pansan Coal Mine," Adv. Civ. Eng., vol. 2020, no. 1, p. 8855335, Jan. 2020, doi: 10.1155/2020/8855335.

[7] Z. Zhu, Z. Yao, J. Nemcik, and J. Han, "Investigation of Overburden Movement and Ground Stress Behaviour in Multiseam Mining," Lithosphere, vol. 2022, no. Special 11, p. 3312379, May 2022, doi: 10.2113/2022/3312379.

[8] M. Huang, S. Jiang, Y. Zhang, Y. Jiang, X. Zhang, and C. Xu, "A new stability analysis model for wet-dry sensitive rocks surrounding underground excavations based on disturbed state concept theory," Int. J. Rock Mech. Min. Sci., vol. 174, p. 105653, Feb. 2024, doi: 10.1016/j.ijrmms.2024.105653.

[9] D. Park and R. L. Michalowski, "Roof stability in deep rock tunnels," Int. J. Rock Mech. Min. Sci., vol. 124, p. 104139, Dec. 2019, doi: 10.1016/j.ijrmms.2019.104139.

[10] E. Hoek and E. T. Brown, "Practical estimates of rock mass strength," Int. J. Rock Mech. Min. Sci., vol. 34, no. 8, pp. 1165–1186, Dec. 1997, doi: 10.1016/S1365-1609(97)80069-X.

[11] Z. T. Bieniawski, Engineering rock mass classifications: a complete manual for engineers and geologists in mining, civil, and petroleum engineering. New York: Wiley, 1989.

[12] H. Kumar et al., "Comparative study of coal rocks compressive behaviors and failure criteria," Arab. J. Geosci., vol. 12, no. 23, p. 710, Dec. 2019, doi: 10.1007/s12517-019-4914-y.

[13] H. Wu, Q. Li, C. Zhu, and P. Tang, "Stability Analysis of Surrounding Rock in Mining Tunnels Based on Microseismic Monitoring and Numerical Simulation," Sustainability, vol. 17, no. 2, p. 630, Jan. 2025, doi: 10.3390/su17020630.

[14] J. Zhao, D. Li, J. Jiang, and P. Luo, "Uniaxial Compressive Strength Prediction for Rock Material in Deep Mine Using Boosting-Based Machine Learning Methods and Optimization Algorithms," Comput. Model. Eng. Sci., vol. 140, no. 1, pp. 275–304, 2024, doi: 10.32604/cmes.2024.046960.

[15] S. Zhao, Y. Chen, W. Xu, J. Xu, and X. Cheng, "Mechanical behaviour and fracture mechanism of coal mine roadway surrounding rock considering seepage field," Front. Mater., vol. 12, p. 1612136, June 2025, doi: 10.3389/fmats.2025.1612136.

[16] X. Liu et al., "Energy driven mechanism of surrounding rock deformation and failure of mining roadway and classified control technology," Sci. Rep., vol. 15, no. 1, p. 15173, Apr. 2025, doi: 10.1038/s41598-025-98452-8.

[17] P. Luo et al., "Evaluation of excavation method on point load strength of rocks with poor geological conditions in a deep metal mine," Geomech. Geophys. Geo-Energy Geo-Resour., vol. 9, no. 1, p. 90, Dec. 2023, doi: 10.1007/s40948-023-00629-w.

[18] Y. Xiao, S. Chen, Z. Wang, L. Liu, and C. Du, "Analyzing the Stability of Rock Surrounding Deep Cross-Tunnels Using a Dynamic Velocity Field," Sustainability, vol. 15, no. 20, p. 15139, Oct. 2023, doi: 10.3390/su152015139.

[19] Z. Wei, W. Yang, Q. Chen, D. Liang, and G. Wu, "Uniaxial compressive strength prediction based on measurement while drilling data: A laboratory study," J. Appl. Geophys., vol. 229, p. 105499, Oct. 2024, doi: 10.1016/j.jappgeo.2024.105499.

[20] X. Tian, L. Dou, S. Hu, X. Ma, and F. Lu, "Risk assessment and mechanism of rock burst for deep soft coal roadways," Sci. Rep., vol. 15, no. 1, p. 7054, Feb. 2025, doi: 10.1038/s41598-025-91619-3.

[21] M. Cai and P. K. Kaiser, "In-situ Rock Spalling Strength near Excavation Boundaries," Rock Mech. Rock Eng., vol. 47, no. 2, pp. 659–675, Mar. 2014, doi: 10.1007/s00603-013-0437-0.

[22] L. Shi and X. Zhang, "An experimental investigation on the failure behaviour of surrounding rock in the stress concentration area of deeply buried tunnels," Bull. Eng. Geol. Environ., vol. 82, no. 12, p. 435, Dec. 2023, doi: 10.1007/s10064-023-03452-5.

[23] N. Barton, "Some new Q-value correlations to assist in site characterisation and tunnel design," Int. J. Rock Mech. Min. Sci., vol. 39, no. 2, pp. 185–216, Feb. 2002, doi: 10.1016/S1365-1609(02)00011-4.

[24] C. Fan, J. Qin, and G. Wang, "Construction Mechanical Characteristics of TBM Pilot and Enlargement Method for Ventilation Tunnel of Wuhai Pumped Storage Power Station," Appl. Sci., vol. 14, no. 5, p. 1829, Feb. 2024, doi: 10.3390/app14051829.

[25] Z. Ni, J. Li, K. Qin, X. Wu, J. Zhu, and S. Zhou, "Experimental study on the mechanical properties and deformation failure characteristics of sandstone under graded equal amplitude cyclic loading and unloading," Sci. Rep., vol. 15, no. 1, p. 28735, Aug. 2025, doi: 10.1038/s41598-025-05052-7.

[26] J. Wang, H. Zhang, S. Qi, H. Bian, B. Long, and X. Duan, "Study on the Strength and Failure Characteristics of Silty Mudstone Using Different Unloading Paths," Materials, vol. 16, no. 14, p. 5155, July 2023, doi: 10.3390/ma16145155.

[27] Y. Fan et al., "Failure characteristics and conditions of rock-coal combination structure with weak layer under dynamic and static stresses," Sci. Rep., vol. 13, no. 1, p. 12410, July 2023, doi: 10.1038/s41598-023-39427-5.